Depth-based multivariate descriptive statistics with hydrological applications

F. Chebana* and T.B.M.J. Ouarda

Canada Research Chair on the Estimation of Hydrometeorological Variables,

INRS-ETE, 490 rue de la Couronne, Quebec (QC),

Canada G1K 9A9

***Corresponding author:** Tel: (418) 654-2542

Fax: (418) 654-2600

Email: fateh.chebana@ete.inrs.ca

November 8th 2010

Abstract

Hydrological events are often described through various characteristics which are generally correlated. To be realistic, these characteristics are required to be considered jointly. In multivariate hydrological frequency analysis, the focus has been made on modelling multivariate samples using copulas. However, prior to this step data should be visualized and analyzed in a descriptive manner. This preliminary step is essential for all of the remaining analysis. It allows to obtain information concerning the location, scale, skewness and kurtosis of the sample as well as outlier detection. These features are useful to exclude some unusual data, to make different comparisons and to guide the selection of the appropriate model. In the present paper we introduce methods measuring these features, and which are mainly based on the notion of depth function. The application of these techniques is illustrated on two real-world streamflow data sets from Canada. In the Ashuapmushuan case study, there are no outliers and the bivariate data are likely to be elliptically symmetric and heavy–tailed. The Magpie case study contains a number of outliers, which are identified to be real observed data. These observations cannot be removed and should be accommodated by considering robust methods for further analysis. The presented depth-based techniques can be adapted to a variety of hydrological variables.

1. Introduction

Extreme hydrological events, such as floods, storms and droughts may have serious economic and social consequences. Frequency analysis (FA) procedures are commonly used for the analysis and prediction of such extreme events. Relating the magnitude of extreme events to their frequency of occurrence, through the use of probability distributions, is the principal aim of FA [*Chow et al.*, 1988].

Generally, several correlated characteristics are required to correctly describe hydrological events. For instance, floods are described by their volume, peak and duration (e.g., Yue et al. [1999]; Ouarda et al. [2000]; Shiau [2003]; Zhang and Singh [2006] and Chebana and Ouarda [2010]). All aspects of univariate FA have already been studied extensively, see e.g. Cunnane [1987] and Rao and Hamed [2000]. On the other hand, multivariate FA has recently attracted increasing attention and the importance of jointly considering all variables characterizing an event was clearly pointed out. Justifications for adopting the multivariate framework to treat extreme events were discussed in several studies (see Chebana and Ouarda [2010] for a summary). For instance, single-variable hydrological FA can only provide limited assessment of extreme events whereas the joint study of the probabilistic characteristics leads to a better understanding of the phenomenon.

In the multivariate hydrological FA literature, the following issues have been addressed: (1) showing the importance and the usefulness of the multivariate framework, (2) selecting the appropriate copula and the marginal distributions and estimating their parameters, (3) defining and studying bivariate return periods, and (4) introducing multivariate quantiles. However, with any statistical analysis, the first stage of the study should be a close inspection of the data. If the data are found appropriate, further analysis of the issues listed above can be undertaken. Hence, exploratory analysis of the data is often the initial stage of any modelling effort that uses that data. It allows to understand the nature of the phenomena that generate the data. It is also useful for model selection and sample comparison. This step of the study is often completely neglected in the multivariate hydrological FA literature. The reason could be the unavailability of the required appropriate tools to carry out this step in a clear and practical manner. Nevertheless, this step is commonly carried out in practice in any univariate hydrological FA study as pointed out by Helsel, et al. [2002]. The development of equivalent tools for the multivariate framework should help promote the use of multivariate FA in hydrological practice.

Exploratory descriptive analysis consists in quantifying and summarizing the properties of the samples and the distributions. Exploratory analysis is useful to guide the selection of the distribution shape and summary statistics are required to characterize the sample or to judge whether the sample is similar enough to some known distribution [Warner, 2008]. For instance, the location, scale, skewness and kurtosis indicate respectively the centrality, dispersion, symmetry and peakedness of the sample. Location and scale are summary statistics of the data whereas the shape of the data can be captured by skewness and kurtosis [*Bickel and Lehmann*, 1975a; b; 1976; 1979]. On the other hand, outliers, as gross errors and inconsistencies or unusual observations, can have negative impacts on the selection of the appropriate distribution as well as on the estimation of the associated parameters. In order to base the inference on the right data set, detection and treatment of outliers are also important ([*Barnett and Lewis*, 1998] and [*Barnett*, 2004]). These concepts are well defined and their computation is straightforward for univariate samples and distributions.

In classical multivariate analysis, several techniques were directly inspired by univariate techniques and developed by analogy (multivariate normal distribution-based, component-wise and moment-based). Techniques that analyse data in a component-wise manner perform badly when variables are mutually dependent. Moment-based methods depend on the existence of moments. For a detailed review of classical multivariate analysis techniques, the reader is referred to Anderson [1984] or Schervish [1987].

Recently developed techniques avoid the above drawbacks by using the multivariate inward-outward ranking of depth functions [*Zuo and Serfling*, 2000b]. Indeed, depth-based techniques are not componentwise, and they are moment-free and affine invariant if the depth function is. These advantages are useful to include distributions such as Cauchy, and also, the obtained results remain the same after standardization. The depth-based ranking enables also numerous outlier detection techniques, which are fundamental in FA. It is important to indicate that, unlike the univariate setting, a multitude of definitions can be proposed for each sample characteristic (such as median and symmetry) in the multivariate context. A key reference in the study of multivariate descriptive statistics is Liu et al. [1999] where most of the above mentioned characteristic are treated. However, each sample feature was subsequently studied separately by a number of authors. For instance, the location was studied by Massé and Plante [2003], Zuo [2003] and Wilcox and Keselman [2004]; scale was treated by Li and Liu [2004], symmetry was the focus of Rousseeuw and Struyf [2004] and Serfling [2006] and kurtosis was addressed by Wang and Serfling [2005]. These studies focused mainly on inferential and asymptotical results. On the other hand, multivariate outlier detection, not discussed in Liu, et al. [1999], was studied recently by Dang and Serfling [2010].

The above features are of particular interest in hydrology since univariate data sets are generally asymmetric [*Helsel et al.*, 2002] and the interest is on the tail of the distribution which is related to kurtosis. In flood FA, Hosking and Wallis [1997] indicated that summary statistics, especially skewness and kurtosis, are often used to judge the closeness of a sample to a target distribution. Regarding outliers, in FA, we are concerned about two particular types of errors: the data may be incorrect and/or the circumstances around the measurement may have changed over time [*Hosking and Wallis*, 1997; *Rao and Hamed*, 2000].

The aim of the present study is to provide and to adapt recent statistical methods to the preliminary analysis and exploration of multivariate hydrological data. The presented methods are mainly based on the statistical notion of depth functions. Depth functions represent convenient tools for the ranking of data in a multivariate context. Chebana and Ouarda [2008] presented a first application of depth functions in the field of hydrology. Note that the multivariate L-moment approach represents also an alternative that could be of interest for the development of multivariate descriptive statistics. This approach is not treated in the present study and could be studied and compared to depth-based approaches in future work. The reader is referred to Serfling and Xiao [2007] for the general multivariate L-moment theory and to Chebana and Ouarda [2007] and Chebana et al. [2009] for applications in hydrology.

The rest of the paper is organized as follows. In section 2, we present the general methodology for exploratory descriptive analysis including graphical tools, measurements of location, dispersion, symmetry, peakedness and outlyingness identification. We apply these concepts to real-world flood data in section 3. Conclusions are presented in section 4. In the appendix, we present a brief summary of the required background elements related to depth-functions.

2. Methodology

In this section, we present the general framework of the exploratory and descriptive multivariate statistical tools. Let $X_1, X_2, ..., X_n \in R^d$ be a *d*-dimensional ($d \geq 1$) sample with size $n \geq d$. Using a given depth function *D*(.), we sort the sample in decreasing order of depth values to obtain $X_{[1]}, X_{[2]}, ..., X_{[n]}$ and we define the "*de-class*" of $X_{[i]}$ as the set of observations with equal depth values, for $i = 1,...,n$. A brief description of depth functions is given in the appendix. Note that, even though, conceptually, any depth function can be used in the following visualisation and analysis efforts, some combinations are not treated here because of the lack of their practical relevance and since their properties are not well known. For instance, bagplots are generally based on Tukey depth and are not studied using the Mahalanobis depth.

2.1 Visualization

Data should be visualized before any analysis can be conducted. In the 2 or 3 dimensional cases, the simplest visualisation tool is the scatter plot. More useful, the bagplot is a generalization of the univariate box-plot to the bivariate setting [*Rousseeuw et al.*, 1999] and is similar to the sunburst-plot presented by Liu et al. [1999]. The bagplot is based on Tukey depth function whereas the sunburst-plot uses either Tukey or Liu depths (given in expressions A1 and A2 respectively). The bagplot is composed by a dark central bag which encircles the 50% deepest points. The Tukey median, defined below in section 2.2, is indicated at the center and a light region delimited by the points included in the central dark bag inflated by a factor 3 is also drawn and called the fence. Points outside this region are considered as statistical outliers. We then link non-outlying points that are outside the dark bag with the Tukey median. These lines have the same role as the whiskers in univariate box plots [*Rousseeuw et al.*, 1999]. The bagplot generally gives indications concerning the distribution of the sample, such as location, dispersion and shape. Note that the sunburst plot presented by Liu et al. [1999] does not contain a fence region and hence the sunburst plot is not considered as a tool to detect outliers. The points outside the fence are considered as extremes rather than outliers. In the present study, we consider a more appropriate approach, given in Section 2.6, to detect outliers.

Another way to visualise data can be obtained using the contours of the depth function. Contours can reveal the shape and structure of multivariate data. Such plots enable direct comparisons of geometry between bivariate data sets. The Tukey depth function is the most used and studied for contour plots.

2.2 Location parameters

A location parameter indicates where most of the data are located. This notion is useful in hydrology since it appears in almost all commonly employed probability distributions. In addition, the location parameter is an important constituent in the index-flood model ([*Hosking and Wallis*, 1993] and [*Chebana and Ouarda*, 2009]).The concept of location is closely related to the center-outward ranking of depth functions. A point maximizing a depth function can be considered as a location parameter, because of the property of "maximality at the center" of depth functions given in the Appendix [*Zuo and Serfling*, 2000b]. In the following, we present several location parameters some of which are well-known, such as the sample mean and the component-wise median.

Sample mean: The simplest and common location parameter is the arithmetic mean:

$$\mu_n = \frac{1}{n}\sum_{i=1}^{n} X_i \tag{1}$$

μ_n is d-dimensional. It corresponds simply to the component-wise arithmetic means.

***α-depth-trimmed-mean* :** For a coefficient $0 \le \alpha \le 1$, the α-depth-trimmed-mean ([*Liu et al.*, 1999] and [*Massé*, 2009]) is a generalization of the sample mean (1). Given a depth function, the α-depth-trimmed-mean can be considered as the sample mean computed from the $100(1-\alpha)\%$ deepest points. Formally, we first define the R^d-valued function ξ_n on $[0,1]$ as:

$$\xi_n(t) = X_{[i]} \quad \text{if} \quad \frac{i-1}{n} < t \le \frac{i}{n} \quad \text{and} \quad \xi_n(0) = X_{[1]} \tag{2}$$

and $\overline{\xi}_n(t)$ as the average over the *de*-class values in which $\xi_n(t)$ is contained. We then define the *DL_n-statistic* as:

$$DL_n = \int_0^1 \overline{\xi}_n(t)\omega(t)\,dt \qquad (3)$$

where $\omega(t)$ is a non negative weight function such that $\int_0^1 \omega(t)\,dt = 1$. The α-depth-trimmed-mean is defined according to a particular function $\omega_\alpha(t)$ given by:

$$\omega_\alpha(t) = 1/(1-\alpha) \quad \text{if } t \in [0, 1-\alpha] \text{ and } \omega_\alpha(t) = 0 \text{ if } t \in (1-\alpha, 1] \qquad (4)$$

If $\alpha = 0$, the α-depth-trimmed-mean is the classical mean given in (1). For $\alpha = 1$, i.e. all observations are trimmed, then DL_n is defined as the deepest point of the sample. For $0 < \alpha < 1$, if $n\alpha$ is an integer, then DL_n is simply $DL_n = \frac{1}{n(1-\alpha)} \sum_{i=1}^{n(1-\alpha)} X_{[i]}$.

The use of the $\alpha\%$ trimmed-mean as a robust estimator in the univariate framework in hydrology was discussed by Ouarda and Ashkar [1998].

Component-wise median: As a direct extension of the univariate median and similarly to the multivariate arithmetic mean, the component-wise median CM_n is defined as:

$$CM_n = \left(med\left(X_{1,1}, X_{2,1}, \dots, X_{n,1}\right); \dots; med\left(X_{1,d}, X_{2,d}, \dots, X_{n,d}\right)\right)' \qquad (5)$$

where *med* is the usual univariate median. Note that CM_n is not affine equivariant.

Depth medians: The following three location parameters are based on depth functions. The labels of these medians are directly taken from their respective depth functions, Tukey, Oja and Liu, given in the appendix. Any other depth function could also be used to define a location median but the above are the most studied in the literature.

We consider the set $E \subseteq R^d$ of points that maximize the considered depth function. The depth median is the centeroïd of the polygon composed by the set of points maximizing the selected depth function [*Massé and Plante*, 2003]. Generally, E is a convex and compact set [*Leon and Massé*, 1993]. Tukey and Oja medians have suitable properties whereas those of Liu median are not studied. The set E corresponding to Tukey median is convex since the half-space depth function is quasi-concave [*Rousseeuw and Ruts*, 1999]. Tukey median is then defined as the center of mass of E [*Massé and Plante*, 2003]. For the Oja median, if n is even, then the set E is a single element according to Oja and Niinimaa [1985].

Spatial median: The spatial median is defined as [*Massé and Plante*, 2003]:

$$SpMed = \frac{1}{n} \arg\min_{x \in R^d} \sum_{i=1}^{n} \left\| x - X_i \right\| \tag{6}$$

where $\|.\|$ is the Euclidean norm and $\arg\min_{t \in A} \varphi(t)$ is the minimiser of the function $\varphi(.)$ over a set A.

In the bivariate case, a numerical study by Massé and Plante [2003] compared all the above mentioned location estimators. The spatial median (6) stands as the best location parameter in terms of robustness and accuracy, followed by Oja and Tukey medians. In a second group, we find the Liu and the component-wise medians in terms of robustness. Trimmed means (for α = 0.05, 0.10 with Tukey and Liu depths) are in a third group, followed finally by the sample mean. Overall, medians were shown to be more robust location parameters than means. Note that except for the Liu and Oja medians, all the above location parameters are computable in higher dimensions, though sometimes under approximations.

2.3 Scale parameters

Scale parameters are useful to measure the dispersion of a distribution or a sample. The scale and location parameters appear in almost all probability distributions employed in hydrology since these distributions should contain at least two parameters. We present two types of multivariate scale parameters: matrix-valued and scalar-valued.

α-trimmed sample dispersion matrix: Given a center-outward ranking of data derived from a given depth function, we first define a general weighted scale matrix [*Liu et al.*, 1999]. The corresponding definition is similar to that of DL_n (given in (3)), except that we replace $\xi_n\left(t\right)$ by the function $S_n\left(t\right)$ defined on the space $\mathrm{M}_d\left(R\right)$ of $d \times d$ real-valued matrices by:

$$\mathbf{S}_n(t) = \left(X_{[i]} - \nu_n\right)\left(X_{[i]} - \nu_n\right)' \quad \text{if } \frac{i-1}{n} < t \le \frac{i}{n}, \quad \text{and } \mathbf{S}_n(0) = \mathbf{0}_{d \times d} \tag{7}$$

where v_n is the sample's deepest point and $\mathbf{0}_{d \times d}$ is the $d \times d$ matrix with null elements. The *weighted scale matrix* is defined by:

$$DS_n = \int_0^1 \overline{\mathbf{S}}_n\left(t\right)\omega\left(t\right)\,dt \tag{8}$$

where $\overline{\mathbf{S}}_\mathbf{n}$ indicates the average of $\mathbf{S}_\mathbf{n}$ over all *de*-classes to which $X_{[i]}$ belongs and ω is the weight function as defined for the α-trimmed mean. The *α-trimmed sample dispersion matrix* is a particular case of DS_n, with ω defined as in (4). Given $0 \le \alpha < 1$, if $n\alpha$ is an integer, the *α-trimmed-dispersion matrix* is given by:

$$DS_n = \frac{1}{n\left(1-\alpha\right)} \sum_{i=1}^{n(1-\alpha)} \overline{\mathbf{S}}_n\left(\frac{i}{n}\right) \tag{9}$$

For $\alpha = 1$, we define DS_n as the zeros matrix and for $\alpha = 0$, it coincides with the usual covariance matrix.

Note that the matrix form of scale enables an easy comparison of dispersion between dimensions and can reveal more information. However, a matrix is not effective for measuring the overall dispersion of the distribution (e.g. [*Liu et al.*, 1999]). We can overcome this problem by taking a norm of the scale matrix (9). Some known matrix norms can be found in Manly [2005].

Scalar form of scale: Scalar values can be seen as an information reduction regarding scales. Hence, it is more appropriate to plot these values as a curve with respect to a given coefficient. We introduce a graphical tool presented in Liu et al. [1999] that measures the dispersion of a multivariate sample. Given a depth function, the function $Sc_n(p)$, $0 \leq p \leq 1$, returns the volume of the central region $C_{n,p}$ composed of the $\lceil np \rceil$ deepest points, where $\lceil a \rceil$ is the smallest integer larger or equal to a.

The plot of the function $Sc_n(p)$ with respect to p is an evaluation of the expansion of $C_{n,p}$ with respect to p. This kind of scale curves is a simple one-dimensional curve describing the scale. It allows also to quantify the evolution of a sample. The curve $Sc_n(.)$ is interpreted as follows: "if the scale curve of a distribution *G* is consistently above the scale curve of another distribution *F*, then *G* has a larger scale than *F*".

2.4 Skewness

Skewness can be defined as a measure of departure from symmetry. Skewness evaluation is important in hydrology since generally univariate distributions are not symmetric and are one-side heavily-tailed [*Helsel et al.*, 2002]. In the multivariate case, there are several types of symmetry, such as: spherical, elliptical, antipodal and angular. Depth-based tools are presented in this section to empirically evaluate each type of symmetry. In the following, we present the definition of each symmetry as well as how it can be evaluated. The definitions are taken from Liu et al. [1999] and Serfling [2006]. All the following types of symmetry have a common feature: the distribution of a centered random vector $X - c$ is invariant under a given transformation and all of them reduce to the usual univariate symmetry.

***Spherical symmetry*:** "The distribution of the random variable *X* is said to be spherically symmetric about the point *c* if the distributions of $(X - c)$ and $\mathbf{U}(X - c)$ are identical, for any orthonormal matrix **U**." Recall that a matrix **U** is orthonormal if and only if $\mathbf{UU}' = \mathbf{U}'\mathbf{U} = I$ where $\mathbf{U}'$ is the transpose of the matrix **U** and *I* is the identity matrix. This kind of symmetry represents a rotation of *X* about c. The probability density function of *X*, when it exists, is then of the form $g\left((x-c)'(x-c)\right)$ for a nonnegative real-valued function *g*. Examples of this kind of distributions include the multivariate versions of the standard normal, the *t* and the logistic distributions.

To evaluate the spherical symmetry, we consider, for a given depth function, the smallest enclosing *d*-sphere that contains the $\lceil np \rceil$ deepest points for $p \in [0,1]$. We denote $Sph(p)$ the proportion of sample points falling in this sphere. The function $Sph(p)$ is increasing and $p \le Sph(p) \le 1$. The area Δ_n between the curve $y = Sph(x)$ and the diagonal line $y = x$ is an indicator of spherical skewness. A perfectly spherical symmetric sample would imply that the curve $Sph(.)$ is close to the diagonal (i.e. $Sph(p) \approx p$) and hence Δ_n is close to zero.

Elliptical symmetry: "The distribution of the random variable *X* is said to be elliptically symmetric about a certain point *c* if there exists a non singular matrix **V** such that **V***X* is spherically symmetric about *c*." The corresponding probability density function of *X* is of the form $|\boldsymbol{V}|^{-1/2} g\left((x-c)'\boldsymbol{V}^{-1}(x-c)\right)$ which includes, for instance, the multivariate normal distribution with a covariance matrix $\Sigma = \boldsymbol{V}'\boldsymbol{V}$. The corresponding contours of the probability density function are indeed of elliptical shape.

To empirically evaluate elliptical skewness, it is suggested in Liu et al. [1999] that we first standardize data using the scale matrix (see Section 2.3) of the $\lceil np \rceil$ deepest points for $p \in [0,1]$. We then proceed on the basis of the transformed data as in spherical symmetry by evaluating *Sph*(*p*) on the transformed set. We finally plot the function *Sph*(*p*) on the transformed data set. The interpretation of the curves associated to the elliptical skewness is similar to that of the spherical skewness.

Antipodal symmetry**:** "The distribution of the random variable X is said to be antipodally symmetric about the point c (if such a point exists) if the distributions of $(X-c)$ and $-(X-c)$ are identical." This symmetry is also called reflective or diagonal and represents the most direct extension of the usual univariate symmetry. The probability density function f in this case is such that $f(x-c) = f(c-x)$.

Given a depth function and a location parameter μ, we consider the reflection of the p^{th} central region $C_{n,p}$ about μ, for p in (0, 1). We denote $Ca(p)$ the proportion of the $\lceil np \rceil$ deepest points falling in the intersection of $C_{n,p}$ and its reflection. By definition we have $0 \leq Ca(p) \leq \lceil np \rceil / n$. An antipodal symmetric sample would suggest that $Ca(p) = \lceil np \rceil / n \approx p$. Thus, we can measure antipodal skewness by evaluating the area between the diagonal line $y = x$ and the curve $y = Ca(x)$, for $x \in [0, 1]$. A larger area corresponds to a larger deviation from antipodal symmetry.

Angular symmetry: "The distribution of the random variable X is said to be angularly symmetric about the point c if, conditional on $X \neq c$, the distributions of $(X-c)/\|(X-c)\|$ and $-(X-c)/\|(X-c)\|$ are identical." One of the features of this symmetry is that if c is a point of angular symmetry, then any hyper-plane passing through c divides the whole space R^d into two half-spaces with probability 0.5 (if the distribution is continuous). More characterizations of angular symmetry can be found in [*Zuo and Serfling*, 2000a].

To measure angular symmetry of a given sample, we first identify the deepest point ν_n according to a given depth function. Then, we evaluate the Tukey depth of the deepest point ν_n with respect to the restricted data in the p^{th} central region $C_{n,p}$ for each $p \in [0,1]$. The deviation of the obtained curve, denoted $h(p)$, from the x axes measures the degree of the antipodal symmetry. The value of Tukey depth of the deepest point should be 0.5 under angular symmetry. The interpretation of the obtained values and curves follows from: " [...] the deviation of the half-space depth at the deepest point from the value 0.5 is a measure of the departure from angular symmetry of the empirical distribution determined by the sample points within each level set" [*Liu et al.*, 1999].

Liu et al. [1999] suggested to consider only the part of the curve with p larger than 0.4 where the curve stabilizes. Note that for small values of p, the curve is based on a small fraction of the data which is not enough for the convergence of the Tukey depth function.

The reader may have noted that these concepts of symmetry are linked together. They can be ranked from more to less restrictive:

$$\begin{array}{c}\text{Spherical}\\\text{symmetry}\end{array} \Rightarrow \begin{array}{c}\text{Elliptical}\\\text{symmetry}\end{array} \Rightarrow \begin{array}{c}\text{Antipodal}\\\text{symmetry}\end{array} \Rightarrow \begin{array}{c}\text{Angular}\\\text{symmetry}\end{array} \qquad (10)$$

In all kinds of symmetry, a point c is required. This point is generally a location parameter. Zuo and Serfling [2000a] studied the performance of some location measures associated to multivariate symmetry.

After having defined and evaluated skewness, it is important to conduct hypothesis testing for symmetry. This represents a current topic of research in the multivariate setting (see for instance

Manzotti et al. [2002], Huffer and Park [2007], Sakhanenko [2008] and Ngatchou-Wandji [2009]). The topic of hypothesis testing is beyond the scope of the present study.

2.5 Kurtosis

Peakedness and tailweight evaluations are important in hydrology as the focus is often on extreme events and the tail of the distribution. These concepts are related to kurtosis which is a measure of the overall spread relative to the spread in the tails. Measuring kurtosis is important in water sciences since extreme events occur in the tail of the distribution (univariate or multivariate) with non negligible probability. Kurtosis is generally defined as a ratio of two scale measures, i.e. scale of the whole data and scale of the central part [*Bickel and Lehmann*, 1979]. We present in this section a number of tools that quantify multivariate kurtosis. The reader is referred to Liu et al. [1999] and Wang and Serfling [2005] for more details.

Lorenz curve of Mahalanobis distance: Given a non-singular scale matrix $\mathbf{S}_n$, such as the one given in (8) or simply the covariance matrix, and a given depth function for which ν_n is the deepest point, we introduce the real-valued functions:

$$L(p) = \frac{\sum_{i=1}^{\lceil np \rceil} Z_i}{\sum_{i=1}^{n} Z_i} \quad \text{and} \quad L^*(p) = \frac{\sum_{i=1}^{\lceil np \rceil} Z_i \Big/ \lceil np \rceil}{\sum_{i=1}^{n} Z_i \Big/ n} \quad \text{for } 0 < p \le 1 \qquad (11)$$

where

$$Z_i = \left(X_{[i]} - \nu_n\right)' \mathbf{S}_n^{-1} \left(X_{[i]} - \nu_n\right), \text{ for } i = 1, 2, \ldots, n \qquad (12)$$

We define $L(0) = L^*(0) = 0$ and we have $L(1) = L^*(1) = 1$. Note that L^* is simply an adjusted formulation of L and each of them represents a ratio of the central variability to the total variability. The functions given in (11) are then plotted and the area corresponding to the surface between the curves $y = L(x)$ or $y = L^*(x)$ and the diagonal line $y = x$ is evaluated. Both areas can be interpreted in the same way: a large area corresponds to a high degree of peakedness and tailweight, and inversely a small area corresponds to heavy shoulders. The curves L^* and L have the same interpretation, but the area computed from L^* should be more pronounced than the one computed from L. Consequently, sample curves can be compared more effectively using L^* than L.

Shrinkage plots: They are based on the shrinkage of the boundary of the pth central region $C_{n,p}$ towards its center by a given fixed coefficient s, $0 < s < 1$ leading to region $C^s_{n,p}$. We then plot the function $a_s(p)$ of the fraction of observations in $C^s_{n,p}$ for fixed s. Liu et al. [1999] indicated that one value of s is enough to conclude and they proposed s = 0.5. For a fixed s, heavier tails correspond to higher values of $a_s(p)$ especially for large p.

Fan plots: A fan plot is a collection of curves used to evaluate kurtosis. It consists in an arbitrary number of curves, each of which is associated with a value $p \in [0,1]$. For a given p, we consider the sub-sample *Sam*(p) formed by the $\lceil np \rceil$ deepest points (in the central region $C_{n,p}$). For $t \in [0,1]$, we denote $C_n(p,t)$ the area of the t^{th} convex hull of *Sam*(p) composed by 100t % of the deepest observations. We define the function $b_p(t)$ for $t \in [0,1]$ by:

$$b_p(t) = \frac{volume\left[C_n(p,t)\right]}{volume\left[C_n(p,1)\right]} \text{ if } C_n(p,1) \neq 0 \text{ and } b_p(t) = 0 \text{ otherwise} \qquad (13)$$

Intuitively, a fan plot may be regarded as a comparison of areas between central (corresponding to low values of p), shoulder (corresponding to middle values of p) and tail regions (corresponding to high values of p). A more spread out fan plot indicates that the corresponding distribution is heavy tailed since $b_p(t)$ becomes smaller. This way to measure kurtosis requires a large amount of data since the data size is reduced in two stages (with p and then with t).

Quantile-based measure: This measure is based on the function $k_C(.)$ proposed by Wang and Serfling [2005] and expressed as :

$$k_C(r) = \frac{V_C\left(\frac{1}{2}-\frac{r}{2}\right)+V_C\left(\frac{1}{2}+\frac{r}{2}\right)-2V_C\left(\frac{1}{2}\right)}{V_C\left(\frac{1}{2}+\frac{r}{2}\right)-V_C\left(\frac{1}{2}-\frac{r}{2}\right)} \quad \text{for} \quad 0<r\leq 1 \text{ and } k_C(0)=0 \qquad (14)$$

where the function $V_C(r)$ is the volume of a central set $C(r)$. The set $C(r)$ is defined as the inner set, with probability r, delimited by contours of a given depth function. Wang and Serfling [2005] used Tukey depth function and indicated that any affine invariant depth function can be used as well. Note that the set $C(r)$ is general with a special case defined on the basis of spatial quantiles. The measure $k_C(r)$ represents the difference of the volumes of two regions A and B divided by the sum of their volumes where $A = C(1/2) - C(1/2 - r/2)$ and $B = C(1/2 + r/2) - C(1/2)$. Note that the boundary associated to the region $C(1/2)$ represents the "shoulders" of the distribution and it separates the "central part" from the corresponding "tail part".

Wang and Serfling [2005] provided indications for the interpretation of the curve $k_C(.)$. They indicated that if the attention is confined to a class of distributions for which either F is unimodal, F is uniform, or $1-F$ is unimodal, then, for any fixed r, a value of $k_C(r)$ near +1 suggests a peakedness, a value near -1 suggests a bowl-shaped distribution, and a value near 0 suggests uniformity.

Increasing values of $k_C(.)$ indicate that the probability mass is greater in the center than in the tails. It is important to mention that, unlike kurtosis measures discussed in the above sub-sections, the quantile-based measure requires some prior knowledge about the distribution of the sample to interpret the obtained curves.

2.6 Outlier detection

Identifying outliers is an important statistical step to analyze data sets as indicated, for instance, by Barnett and Lewis [1978] in the univariate as well as in the multivariate settings. Outlier detection in hydrologic data is a common problem which has received considerable attention in the univariate framework.

In the multivariate setting, outlyingness functions are defined and employed to detect outliers. Values of these functions usually range in the interval [0, 1]. They measure outlyingness of a certain point with respect to the entire sample. An outlyingness value near 1 indicates high outlyingness, and inversely a value near 0 indicates centrality. In order to determine whether an observation is an outlier or not, it is required to define a threshold, i.e. the minimum outlyingness value from which a datum is considered to be an outlier. In the following we present the most promising and recently developed outlying functions, based on depth functions and given in Dang and Serfling [2010].

Outlyingness: A depth outlyingness is a transformation of a depth function for a given distribution F and $x \in R^d$. The followings are studied in Dang and Serfling [2010]:

Half-space: $$O_{HD}(x,F) = 1 - 2HD(x,F) \quad (15)$$

Mahalanobis: $$O_{MD}(x,F) = d^2_{A(F)}(x,\mu(F)) \Big/ \left[1 + d^2_{A(F)}(x,\mu(F))\right] \quad (16)$$

Projection: $$O_{PD}(x,F) = PD(x,F) \Big/ \left[1 + PD(x,F)\right] \quad (17)$$

where $HD(.,F)$, $d^2_{A(F)}(.,\mu(F))$ and $PD(.,F)$ are given respectively in (A1), (A3) and (A6) and $\mu(F)$ is a location measure and $A(F)$ is a nonsingular matrix scale measure;

Spatial: $$O_S(x,F) = \left\| E\left(Sign(x - X)\right)\right\| \quad (18)$$

Spatial Mahalanobis: $$O_{SM}(x,F) = \left\| E\left[Sign\left(\mathbf{C}^{-1/2}(x - X)\right)\right]\right\| \quad (19)$$

where $\|.\|$ is the Euclidean norm, X is F-distributed and $Sign(.)$ is the multidimensional sign function given by:

$$Sign(x) = x/\|x\| \ \text{ if } x \neq 0 \quad \text{and} \quad Sign(0) = 0 \qquad (20)$$

and $\mathbf{C}$ is any affine invariant symmetric positive definite $d \times d$ matrix. The matrix $\mathbf{C}$ could be the classical covariance matrix or the matrix obtained as the minimum covariance determinant [*Rousseeuw and Van Driessen*, 1999].

Threshold: Selection of the appropriate threshold is an important step in outlier detection. It is related to false positive and true positive rates. The arbitrary *false positive rate*, denoted α_n, is the proportion of non-outliers misidentified as outliers. This constant is closely related to the *true positive rate* ε_n, which represents the real theoretical proportion of outliers (called also contaminants). Ideally, α_n has to be small compared to ε_n. Dang and Serfling [2010] fixed a ratio of false outliers $\delta = \alpha_n / \varepsilon_n$ and then used an additional coefficient $\beta = \varepsilon_n \sqrt{n}$, to define a threshold as the (1-α_n)-quantile of the outlyingness values :

$$\lambda_n = F^{-1}_{O(X,F)}\left(1-\alpha_n\right) = F^{-1}_{O(X,F)}\left(1-\delta\varepsilon_n\right) = F^{-1}_{O(X,F)}\left(1-\beta\delta/\sqrt{n}\right) \qquad (21)$$

The following example is illustrated in Dang and Serfling [2010]. By putting δ = 0.1, the ratio of false outliers is about 10% among the allowed ones. Assume that we allowed for $n\varepsilon_n = 15$ true outliers, the constant β takes the value $\beta = n\varepsilon_n / \sqrt{n} = 15/\sqrt{100} = 1.5$ for n = 100. Hence, $\lambda_n = F^{-1}_{O(X,F)}\left(1-0.15/\sqrt{n}\right) = F^{-1}_{O(X,F)}\left(0.985\right)$ for n = 100 corresponds to the 0.985-quantile of the outlyingness values.

These thresholds are given explicitly for the multivariate normal distribution. Since, these thresholds are not available in general, those of the normal distribution can be employed as approximations. For a multivariate sample from a multivariate normal distribution Φ, the theoretical threshold λ_n is given explicitly for the Malahanobis, half-space and projection outlyingness functions of Dang and Serfling [2010]. Supposing that $\beta\delta/\sqrt{n} \in [0,1]$ and that the variable X is standard normally distributed, then the threshold given in (21) is given more explicitly as:

$$
\begin{aligned}
\lambda_n &= \frac{T(d,\alpha_n)}{1+T(d,\alpha_n)} && \text{for the Mahalanobis outlyingness} \\
\lambda_n &= 2\Phi\left(T(d,\alpha_n)\right)-1 && \text{for the halfspace outlyingness} \\
\lambda_n &= \frac{T(d,\alpha_n)}{\Phi^{-1}(3/4)+T(d,\alpha_n)} && \text{for the projection outlyingness}
\end{aligned}
\qquad (22)
$$

where $T(d,\alpha)=\sqrt{\left(\chi_d^2\right)^{-1}(1-\alpha)}$ with $\left(\chi_d^2\right)^{-1}$ is the inverse cumulative distribution function of the chi-square distribution with d degrees of freedom.

For the spatial and spatial Mahalanobis, normal thresholds are not available. Note that it is also convenient to define thresholds for each outlyingness function on the basis of the empirical quantile of the outlyingness values.

3. Applications

In the following, the notions and methods introduced in Section 2 are applied to two real-world hydrological data sets. The first one is given in details whereas in the second one, we focus on outlier detection. All the methods presented in Section 2 are implemented in the Matlab environment [*MathWorks*, 2008] for the bivariate setting. Few methods, such as those based on the Mahalanobis distance, can be applied to higher dimensions.

3.1 Ashuapmushuan case study

The data set used in this case study is taken from Yue et al. [1999] and concerns floods in the Ashuapmushuan basin located in the province of Québec, Canada. The flood annual observations of flood peaks (Q), durations (D) and volumes (V) were extracted from a daily streamflow data set from 1963 to 1995. The gauging station, with identification number 061901, is near the outlet of the basin, at latitude 48.69°N and longitude 72.49°W. In this region floods are caused by high spring-snowmelt.

To allow comparisons, we considered the study of all three combination series (Q, V), (D, V) and (Q, D) by all presented methods. In all parts of the analysis, except for outlier detection, we considered four depth functions: Tukey, Oja, Mahalanobis and Liu which are given respectively in (A1), (A2), (A4) and (A5). Note that results were produced for the three bivariate series using the four depth functions. However, the four depth functions lead to practically identical results for each series. Therefore, in the following we only present results based on the Tukey depth function. A sample's depth values are essential for the analysis since almost all tools presented above are depth-based. The corresponding depth values for the series (Q, V) are given in Table 1 as a selected example.

Displaying data

Bagplots and contour plots, based on Tukey depth, are presented in Figures 1a,b respectively. The Tukey depth function is the most used for bagplots and contour plots. We observe the orientation of the bags which indicates the positive correlation between Q and V. We also observe that more data are concentrated in the center and that the extreme observations, with high V and relatively small Q, are located outside the fence of the (Q, V) plot. All three series are unimodal, both (Q, V) and (D, V) are positive dependent whereas (Q, D) shows no clear dependence. This is in agreement with the multivariate flood FA literature (e.g. [*Yue et al.*, 1999] and [*Zhang and Singh*, 2006]). The series (Q, V) seems more concentrated and tight than the other two. The contours of (Q, D) are more circular and more distant compared to those of the (Q, V) and (D, V) series. Note that the points outside the fence of (Q, V) and (D, V) in Figure 1b (left and middle) correspond to the floods of 1994 and 1974 respectively. They have the smallest depth values. As indicated previously, they cannot be considered as outliers at this stage of the analysis but can be seen as extremes.

Location parameters

All location parameters presented in Section 2.2 are obtained in the bivariate setting. Location parameters are indicated in Figure 2, both within the scatter plot and separately in a zoomed plot. The corresponding values are given in Table 2. Generally, all location parameters are located in the center of the sample. We observe that locations based on the mean are slightly influenced by the extreme values of the sample, for instance, in the series (Q, D). This result is in agreement with the study by Massé and Plante [2003] where the authors recommend, on the basis of accuracy and robustness, the use of spatial median followed by Oja and Tukey medians.

Scale parameters

The α-trimmed dispersion matrix, given in (8), is easily computed for any multivariate setting. Corresponding values associated to each series are presented in Table 3 for $\alpha = 0.00$, 0.05 and 0.10. For a given series, all matrices are in the same order of magnitude with a slight decrease with respect to α. Values in the matrices corresponding to (Q, V) are larger than those of (D, V) and the smallest are those of (Q, D). All values in the dispersion matrices are positive except for those representing the covariance between Q and D. This was already indicated when displaying data and is again in agreement with the hydrological literature (e.g. [*Yue et al.*, 1999] and [*Zhang and Singh*, 2006]).

In addition, Figure 3 presents, for each series, the function $Sc_n(p)$ with respect to p of the volume of the pth central region $C_{n,p}$. We observe that (Q, V) is more dispersed than both (D, V) and (Q, D) since $Sc_n(p)$ corresponding to (Q, V) is larger for any fixed p. This can be partially explained by comparing the magnitudes of volumes ($\approx 10^4$), flood peaks ($\approx 10^3$) and durations ($\approx 10^1$). Moreover, the variances of the marginal variables differ greatly: the variance of V (σ^2 = 1.55e+008) is larger than the variance of Q (σ^2 = 1.29e+005) and the variance of D (σ^2 = 211.30). The variability induced by D is included in both Q and V because they are evaluated on D. This is in concordance with matrix dispersion given in Table 3. These findings, both with matrices and scalars, confirm what was previously revealed from bagplots and contour plots in Figure 1.

Skewness measures

The measures of the four kinds of symmetry, presented in Section 2.4, are applied on each one of the three series. Figure 4 illustrates the curves of the four skewness measures. We notice that the $(D,\ V)$ sample is the closest to spherical symmetry with a small volume $\Delta_n = 0.09$ (Figure 4a). Results from Figure 4b suggest that the (Q, V), (D, V) and (Q, D) distributions are likely to be elliptically symmetric, since $Sph_n(p)$ is very close to the diagonal with a very small Δ_n. This can be confirmed with the bagplots and contour plots of Figures 1a and 1b respectively. Regarding antipodal skewness, Figure 4c shows that all the considered series seem to be symmetric since the obtained curves are similar to those in Figure 14 in Liu et al. [1999] and are already elliptically symmetric. Among the three series, (Q, D) is the closest to angular symmetry since the function $h(p)$ converges to 0.5 for p larger than 0.4 (Figure 4d). Hence, the three series seem to be elliptically symmetric. Note that the procedure treats the whole distribution including copula and margins. The univariate skewness coefficient values are 0.978, 0.522 and 0.286 respectively for D, V

and Q. Since these values are significantly non null, the corresponding marginal distributions are positively skewed. In contexts similar to the present one, the so-called meta-elliptical distributions could be a reasonable model to consider. In the statistical literature, meta-elliptical copulas are studied by Abdous et al. [2005] and applied in hydrology by Wang et al. [2010]. Meta-elliptical distributions allow margin variables to follow different distributions. It is advisable to check the significance of this symmetry by using statistical tests given in the references provided in Section 2.4. These findings are useful to guide the selection of the appropriate distribution for further analysis.

Kurtosis parameters

For all three series (Q, V), (D, V) and (Q, D), the curves to evaluate kurtosis are presented in Figure 5. The functions L and L^* defined in (11) are presented in Figures 5a,b respectively. Clearly, as expected, L^* is more distinctive than L. Hence, the series (Q, V) represents the most peaked sample, followed by (Q, D) and then by (D, V) according to L^*.

Shrinkage plots, in Figure 5c, are very similar and do not allow to compare the various series, apart that all the three series are heavy-tailed. However, fan plots indicate again that (Q, V) is the most peaked series (Figure 5d). As explained in Section 2.5, quantile-based curves, provided in Figure 5e, do not reveal indications concerning kurtosis for the studied series since they require some information regarding the generating distribution.

Overall, we conclude that (Q, V) is the most peaked series and that the L^*-based kurtosis measure seems to be the best option since it is simple, distribution-free and able to distinguish between kurtosis of distributions. Therefore, the appropriate distribution candidates should be heavy-tailed as expected.

Outlier detection

We evaluated spatial and both depth-based Mahalanobis and Tukey outlyingness functions for the three series. The results are presented in Table 4. The corresponding thresholds are obtained by selecting the values discussed in Section 2.6: that is the ratio of false outliers $\delta = 0.1$, the true number of outliers $n\varepsilon_n = 5$ corresponding to approximately 15% of the sample, and the constant β $\beta = n\varepsilon_n / \sqrt{n} = 0.8704$ for n = 33. Hence, from expression (21), $\lambda_n = F^{-1}_{O(X,F)}(0.985)$ which corresponds to the 0.985-quantile of the outlyingness values.

Table 4 illustrates the normal and empirical thresholds for each series and each outlyingness function as well as the corresponding detected outliers as years. The results show that there is no outlier for the three series on the basis of the empirical thresholds using the three kinds of outlyingness. However, the normal thresholds are not convenient in the present case. They lead to very small thresholds for Mahalanobis and very high thresholds for Tukey. The reason could be the short sample size of the series which does not allow for appropriate approximations. Furthermore, it is well documented that flood series are not normally distributed. Note that the (Q, V) and (D, V) of the years 1974 and 1994 are not detected as outliers even by relaxing the coefficients δ and $n\varepsilon_n$.

3.2 Magpie case study

The data series related to the second case study consists in daily natural streamflow measurements from the Magpie station (reference number 073503). This station is located at the discharge of the Magpie Lake in the Côte-Nord region in the province of Québec, Canada. Data are available from 1979 to 2004. In this case study we focus on outlier detection for the flood peak Q and the flood volume V series. The corresponding Tukey depth and the outlyingness values are reported in Table 5.

To obtain the threshold that the outlyingness of an outlier exceeds, we considered $\delta = 0.15$ as the ratio of false outliers and $n\varepsilon_n = 5$ as the number of true outliers. Therefore, from expression (21), the threshold corresponds to the empirical 97%-quantile of the outlyingness values. Numerically, the obtained thresholds are respectively 0.9231, 0.8676 and 0.9462 for O_{HD}, O_{MD} and O_S. Consequently, the flood of 1981 is detected by all the measures as outlier, whereas 1987 is detected only by O_{HD} and has the second highest outlying value by both O_{MD} and O_S. The measure O_{HD} detects several other outliers, such as 1999 and 2002, with the same outlyingness value (equal to the threshold). However, if a quantile of order higher than 97% is considered, by modifying the parameters related to the threshold, then O_{HD} will not detect any outliers. Note that according to Dang and Serfling [2010], the O_{HD} measure is not recommended.

To explain these outliers, hydrological characteristics were derived and the corresponding meteorological data were examined. These data were extracted from Environment Canada's Web site (www.climat.meteo.gc.ca/climateData/canada_f.html). The hydrograph of the year 1981 is characterized by very high V and Q whereas 1987 seems to correspond to a dry year since the flow was the lowest during the spring season and has the lowest V and Q values in the series. For 1981 there was an important amount of snow in early winter (October to January) followed by thaw and rain during February-March. In comparison to the previous and following years, 1987 was characterised by a warm end of winter and a very cold and less rainy fall. Hence, snow melted earlier compared to other years. The flood of 1999 is characterised by a high V, although lower than the one corresponding to 1981. The year 1999 was characterised by an important quantity of snow on the ground with high temperatures in March. The observed hydrograph of 2002 contains two peaks: the first one is characterised by a high magnitude while the second one is smaller and occurs later in the summer. This year was particular with a very cold winter and a large amount of snow on the ground until early May. In conclusion, the flows of the above detected years seem unusual but are actually observed and do not correspond to incorrect measurements or changes over time in the circumstances under which the data were collected. Hence, these observations should be kept and employed for further analysis. However, it is recommended to use robust statistical methods to avoid sensitivity of the obtained results to outliers.

The Tukey median and the arithmetic mean are evaluated. We observe that the median corresponds to the year 1980 with Q = 847.72 and V = 2216.22. The bivariate mean vector is (Q = 859.15, V = 2138.70). After removing any of the above outliers, the mean changes significantly whereas the median remains the same. For instance, the mean becomes (835.25, 2067.89) after removing the 1981 outlier. This result illustrates the effect of the detected outliers on the mean which is not the case for the median. Since the detected outliers represent actual observations, it is not advised to remove them. In that case, the median is recommended as a location measure. For further analysis, robust methods and measures are recommended for this data set.

4. Conclusions

The techniques and methods presented in the present paper constitute the first step in a multivariate frequency analysis. In the present paper, several features of the sample are treated, such as location, scale, skewness, kurtosis and outlier detection. The methods discussed in the present paper are superior to the classical multivariate methods based on moments, the assumption of normality, and componentwise techniques. These recent methods, mainly based on the notion of depth function, are moment-free, not normally-based and affine invariant (if the depth function is). This preliminary step of the analysis is useful for the modeling of hydrological variables and for risk evaluation. It allows to screen the data, to guide the selection of the appropriate model and to make comparisons of multivariate samples. The methods discussed in the present paper were applied to flood data from the Ashuapmushuan and Magpie data sets in the province of Québec, Canada. These methods can also be adapted and applied to other hydrometeorelogical variables such as storms, heat waves and draughts.

The findings related to the first case study of the Ashuapmushuan basin show that there are no outliers and the data are likely to be elliptically symmetric and heavy–tailed. Therefore, the appropriate multivariate distribution should be in a class with similar features. The second case study of the Magpie station contains a number of outliers which are checked to be real observed data. Therefore, they cannot be removed from the sample and robust methods should be adopted for further analysis.

Acknowledgments

Financial support for this study was graciously provided by the Natural Sciences and Engineering Research Council (NSERC) of Canada and the Canada Research Chair Program. The authors thank Pierre-Louis Gagnon for his assistance. The authors wish to thank the Editor and three anonymous reviewers for their useful comments which led to considerable improvements in the paper.

Bibliography

Abdous, B., C. Genest, and B. Rémillard (2005), Dependence Properties of Meta-Elliptical Distributions, in *Statistical Modeling and Analysis for Complex Data Problems*, edited by P. Duchesne and B. RÉMillard, pp. 1-15, Springer US.

Aloupis, G., C. Cortés, F. Gómez, M. Soss, and G. Toussaint (2002), Lower bounds for computing statistical depth, *Computational Statistics and Data Analysis*, *40*(2), 223-229.

Anderson, T. W. (1984), *An introduction to multivariate statistical analysis*, 2nd ed., 675 pp., Wiley, New York.

Barnett, V., and T. Lewis (1978), *Outliers in statistical data*, Reprint ed., 365 pp., Wiley, Chichester.

Barnett, V., and T. Lewis (1998), *Outliers in statistical data*, 3rd ed., 584 pp., Wiley, Chichester [etc.].

Barnett, V. (2004), *Environmental statistics : methods and applications*, xi, 293 p. pp., J. Wiley, Chichester, England ; Hoboken, N.J.

Bickel, P. J., and E. L. Lehmann (1975a), Descriptive statistics for nonparametric models. II. Location, *Ann. Statist.*, *3*(5), 1045--1069.

Bickel, P. J., and E. L. Lehmann (1975b), Descriptive statistics for nonparametric models. I. Introduction, *Ann. Statist.*, *3*(5), 1038-1044.

Bickel, P. J., and E. L. Lehmann (1976), Descriptive statistics for nonparametric models. III. Dispersion, *Ann. Statist.*, *4*(6), 1139-1158.

Bickel, P. J., and E. L. Lehmann (1979), Descriptive statistics for nonparametric models. IV. Spread, in *Contributions to statistics*, edited by Reidel, pp. 33-40, Dordrecht.

Caplin, A., and B. Nalebuff (1991a), Aggregation and social choice - a mean voter theorem, *Econometrica*, *59*(1), 1-23.

Caplin, A., and B. Nalebuff (1991b), Aggregation and imperfect competition - on the existence of equilibrium, *Econometrica*, *59*(1), 25-59.

Caplin, A., Nalebuff, B. (1988), On 64%-majority rule, *Econometrica*, *56*, 787-814.

Chebana, F., and T. B. M. J. Ouarda (2007), Multivariate L-moment homogeneity test, *Water Resources Research*, *43*(8).

Chebana, F., and T. B. M. J. Ouarda (2008), Depth and homogeneity in regional flood frequency analysis, *Water Resources Research*, *44*(11).

Chebana, F., and T. B. M. J. Ouarda (2009), Index flood-based multivariate regional frequency analysis, *Water Resources Research*, *45*(10).

Chebana, F., T. B. M. J. Ouarda, P. Bruneau, M. Barbet, S. El Adlouni, and M. Latraverse (2009), Multivariate homogeneity testing in a northern case study in the province of Quebec, Canada, *Hydrological Processes*, *23*(12), 1690-1700.

Chebana, F., and T. B. M. J. Ouarda (2010), Multivariate quantiles in hydrological frequency analysis, *Environmetrics*, *in press*.

Chow, V. T., D. R. Maidment, and L. R. Mays (1988), *Applied Hydrology*, 572 pp., McGraw-Hill, New York.

Cunnane, C. (1987), Review of statistical models for flood frequency estimation.

Dang, X., and R. Serfling Nonparametric depth-based multivariate outlier identifiers, and masking robustness properties, *Journal of Statistical Planning and Inference*.

Dang, X., and R. Serfling (2010), Nonparametric depth-based multivariate outlier identifiers, and masking robustness properties, *Journal of Statistical Planning and Inference*, *140*(1), 198-213.

Ghosh, A. K., and P. Chaudhuri (2005), On maximum depth and related classifiers, *Scandinavian Journal of Statistics*, *32*(2), 327-350.

Helsel, D. R., R. M. Hirsch, and Geological Survey (U.S.) (2002), Statistical methods in water resources, edited, U.S. Geological Survey, [Reston, Va.].

Hosking, J. R. M., and J. R. Wallis (1993), Some statistics useful in regional frequency analysis, *Water Resources Research*, *29*(2), 271-281.

Hosking, J. R. M., and J. R. Wallis (1997), *Regional Frequency Analysis: An Approach Based on L-Moments*, 240 pp., Cambridge University Press, Cambridge.

Huffer, F. W., and C. Park (2007), A test for elliptical symmetry, *Journal of Multivariate Analysis*, *98*(2), 256-281.

Leon, C. A., and J. C. Massé (1993), A simplex Oja median - existence, uniqunes, stability, *Canadian Journal of Statistics*, *21*(4), 397-408.

Li, J., and R. Y. Liu (2004), New nonparametric tests of multivariate locations and scales using data depth, *Statistical Science*, *19*(4), 686-696.

Liu, R. Y. (1990), On a notion of data depth based on random simplices, *Annals of Statistics*, *18*(1), 405-414.

Liu, R. Y., and K. Singh (1993), A quality index based on data depth and multivariate rank-tests, *Journal of the American Statistical Association*, *88*(421), 252-260.

Liu, R. Y. (1995), Control charts for multivariate processes, *Journal of the American Statistical Association*, *90*(432), 1380-1387.

Liu, R. Y., J. M. Parelius, and K. Singh (1999), Multivariate analysis by data depth: Descriptive statistics, graphics and inference, *Annals of Statistics*, *27*(3), 783-858.

Manly, B. F. J. (2005), *Multivariate statistical methods, a primer*, 3rd ed., 214 pp., Chapman & Hall/CRC, Boca Raton.

Manzotti, A., F. J. Prérez, and A. J. Quiroz (2002), A statistic for testing the null hypothesis of elliptical symmetry, *Journal of Multivariate Analysis*, *81*(2), 274-285.

Massé, J. C., and J. F. Plante (2003), A Monte Carlo study of the accuracy and robustness of ten bivariate location estimators, *Computational Statistics and Data Analysis*, *42*(1-2), 1-26.

Massé, J. C. (2009), Multivariate trimmed means based on the Tukey depth, *Journal of Statistical Planning and Inference*, *139*(2), 366-384.

MathWorks (2008), MATLAB Version 7.6.0.324, edited, MathWorks, Inc., , Natick, MA.

Mizera, I., and C. H. Müller (2004), Location-scale depth, *Journal of the American Statistical Association*, *99*(468), 949-966.

Ngatchou-Wandji, J. (2009), Testing for symmetry in multivariate distributions, *Statistical Methodology*, *6*(3), 230-250.

Oja, H. (1983), Descriptive statistics for multivariate distributions, *Statistics and Probability Letters*, *1*(6), 327-332.

Oja, H., and A. Niinimaa (1985), Asymptotic Properties of the Generalized Median in the Case of Multivariate Normality, *Journal of the Royal Statistical Society. Series B (Methodological)*, *47*(2), 372-377.

Ouarda, T. B. M. J., and F. Ashkar (1998), Effect of trimming on LP III flood quantile estimates, *Journal of Hydrologic Engineering*, *3*(1), 33-42.

Ouarda, T. B. M. J., M. Hache, P. Bruneau, and B. Bobee (2000), Regional flood peak and volume estimation in northern Canadian basin, *Journal of Cold Regions Engineering*, *14*(4), 176-191.

Rao, A. R., and K. H. Hamed (2000), *Flood Frequency Analysis*, 376 pp., CRC Press, Boca Raton.

Rousseeuw, P. J., and I. Ruts (1996), Bivariate location depth, *Applied Statistics-Journal of the Royal Statistical Society Series C*, *45*(4), 516-526.

Rousseeuw, P. J., and I. Ruts (1999), The depth function of a population distribution, *Metrika*, *49*(3), 213-244.

Rousseeuw, P. J., I. Ruts, and J. W. Tukey (1999), The bagplot: A bivariate boxplot, *American Statistician*, *53*(4), 382-387.

Rousseeuw, P. J., and K. Van Driessen (1999), Fast algorithm for the minimum covariance determinant estimator, *Technometrics*, *41*(3), 212-223.

Rousseeuw, P. J., and A. Struyf (2004), Characterizing angular symmetry and regression symmetry, *Journal of Statistical Planning and Inference*, *122*(1-2), 161-173.

Sakhanenko, L. (2008), Testing for ellipsoidal symmetry: A comparison study, *Computational Statistics and Data Analysis*, *53*(2), 565-581.

Schervish, M. J. (1987), A Review of Multivariate Analysis, *Statistical Science*, *2*(4), 396-413.

Serfling, R. (2006), Multivariate symmetry and asymmetry, in *Encyclopedia of Statistical Sciences*, edited by S. Kotz, N. Balakrishnan, C. B. Read and B. Vidakovic, pp. 5338-5345, Wiley.

Serfling, R., and P. Xiao (2007), A contribution to multivariate L-moments: L-comoment matrices, *Journal of Multivariate Analysis*, *98*(9), 1765-1781.

Shiau, J. T. (2003), Return period of bivariate distributed extreme hydrological events, *Stochastic Environmental Research and Risk Assessment*, *17*(1-2), 42-57.

Tukey, J. W. (1975), Mathematics and the picturing of data, paper presented at Proceedings of the International Congress of Mathematicians, SIAM, Philadelphia, Vancouver

Wang, J., and R. Serfling (2005), Nonparametric multivariate kurtosis and tailweight measures, *Journal of Nonparametric Statistics*, *17*(4), 441-456.

Wang, X., M. Gebremichael, and J. Yan (2010), Weighted likelihood copula modeling of extreme rainfall events in Connecticut, *Journal of Hydrology*, *390*(1-2), 108-115.

Warner, R. M. (2008), *Applied statistics : from bivariate through multivariate techniques*, xxvi, 1101 p. pp., SAGE Publications, Thousand Oaks, Calif.

Wilcox, R. R., and H. J. Keselman (2004), Multivariate location: Robust estimators and inference, *Journal of Modern Applied Statistical Methods*, *3*(1), 2-12.

Yue, S., T. B. M. J. Ouarda, B. Bobée, P. Legendre, and P. Bruneau (1999), The Gumbel mixed model for flood frequency analysis, *Journal of Hydrology*, *226*(1-2), 88-100.

Zhang, L., and V. P. Singh (2006), Bivariate flood frequency analysis using the copula method, *Journal of Hydrologic Engineering*, *11*(2), 150-164.

Zuo, Y., and R. Serfling (2000a), On the performance of some robust nonparametric location measures relative to a general notion of multivariate symmetry, *Journal of Statistical Planning and Inference*, *84*(1-2), 55-79.

Zuo, Y., and R. Serfling (2000b), General notions of statistical depth function, *Annals of Statistics*, *28*(2), 461-482.

Zuo, Y. J. (2003), Finite sample tail behavior of multivariate location estimators, *Journal of Multivariate Analysis*, *85*(1), 91-105.

Appendix: brief presentation of depth functions

The main aim of introducing depth functions was to define multivariate extensions of the rank and order notions. Tukey [1975] presented pioneering work in this direction by proposing the half-space depth function. Several types of depth functions were defined later then standardized and classified by Zuo and Serfling [2000b]. A depth function $D(x; F)$, defined for a given cumulative distribution function F on R^d $(d \geq 1)$ and x in R^d, is any bounded and nonnegative function that meets the following properties:

i. *Affine invariance*: the depth of a point $x \in R^d$ should not depend on the underlying coordinate system or, in particular, on the scales of the underlying measurements. That is, $D(Ax+b; F_{AX+b}) = D(x; F_X)$ holds for any random vector X in R^d, any $d \times d$ nonsingular matrix A and any d-vector b;

ii. *Maximality at center*: for a distribution having a uniquely defined center, the depth function should attain its maximum value at this center;

iii. *Monotonicity relative to deepest point*: as a point $x \in R^d$ moves away from the deepest point along any fixed ray through the center, the depth at x should decrease monotonically;

iv. *Vanishing at infinity*: the depth of a point x should be close to zero as the corresponding norm $\|x\|$ approaches infinity.

The following depth functions have received more attention in the literature [*Zuo and Serfling*, 2000b]:

1. **Tukey depth (called also the Half-space depth):** Given a probability P on R^d and $x \in R^d$, the *Half-space depth* [*Tukey*, 1975], noted *HD*, is given by:

$$HD(x;P) = \inf\{P(H): H \text{ a closed halfspace that contains } x\} \qquad \text{(A1)}$$

The empirical *half-space* depth function is defined by replacing the probability function *P*(*H*) by the proportion of sample observations falling into a half-space *H*. An illustration based on a simple example is given in Figure 6. The depth value of θ is the minimum number of observations falling in the half-spaces (here 2) divided by the sample size 9. Note that θ does not belong to the sample.

2. **Oja depth (called also the Simplicial volume depth):** The *Simplicial volume depth* [*Oja*, 1983], noted *SVD*, is given through the expression:

$$SVD(x,F) = \left(1 + E\left[\Delta\left(S_n\left[x, X_1, ..., X_d\right]\right)\right]\right)^{-1} \quad \text{for} \quad x \in R^d \qquad \text{(A2)}$$

where $\Delta\left(S_n\left[x, x_1, ..., x_d\right]\right)$ is the volume of the closed *d-simplex* $S_n\left[x, x_1, ..., x_d\right]$ formed by the points $x, x_1 ..., x_d \in R^d$. A *d-simplex* is defined as the convex hull of these points. This is a *d-dimensional* generalization of triangles.

3. **Mahalanobis depth**: We introduce the *Mahalanobis* distance:

$$d_A^2(x, y) = (x - y)' A^{-1} (x - y) \qquad \text{(A3)}$$

where $x, y \in R^d$ are column vectors and *A* is any semi-definite-positive matrix. Given a distribution *F*, a scatter measure *A(F)* and a location parameter *μ(F)*, the Mahalanobis depth, noted *MD*, is:

$$MD(x,F) = \left(1 + d_{A(F)}^2\left(x, \mu(F)\right)\right)^{-1} \qquad \text{(A4)}$$

4. **Liu depth (called also the Simplicial depth) :** The *Simplicial depth* [*Liu*, 1990], noted *SD*, of $x \in R^d$ with respect to a distribution *F* is given by:

$$SD(x,F) = P_F\left\{x \in S_n\left[X_1, ..., X_{d+1}\right]\right\} \qquad \text{(A5)}$$

where S_n is as defined above and $X_i \sim F, \ \ i = 1,...,d+1$.

5. **Projection depth**: For a given distribution F of a variable X, we define $F_{u'X}$ as the univariate distribution of the variable $u'X$. Then, given a location and a scatter parameters $\mu(.)$ and $\sigma(.)$, the *projection depth* $PD(.)$ is defined as:

$$PD\left(x,F\right) = \sup_{\|u\|=1} \left| \left(u'x' - \mu\left(F_{u'X}\right)\right) \sigma^{-1}\left(F_{u'X}\right) \right| \qquad \text{(A6)}$$

where $\|.\|$ is the Euclidian norm. The empirical version of PD is obtained by substituting the location and scale measures $\mu(.)$ and $\sigma(.)$ with their estimations, and $F_{u'X}$ by the empirical distribution of the sample $\left\{u'X_1, u'X_2, ..., u'X_n\right\}$.

The computation of depth functions is generally not straightforward and requires specific algorithms. For instance, Rousseeuw and Ruts [1996] and Aloupis et al. [2002] developed algorithms for the computation of the half-space and the simplicial depth functions. The Mahalanobis depth is among the simplest ones to evaluate. However, computational algorithms for the projection depth are not available yet.

Depth functions are applied in several fields such as in econometric and social studies [*Caplin and Nalebuff*, 1991a; b; 1988]. Liu and Singh [1993] and Liu [1995] employed depth functions in industrial quality control. Recently, the depth-based approach proposed by Chebana and Ouarda [2008] improved the performance of Canonical Correlation Analysis in the context of regional flood frequency analysis. Depth functions were also investigated in nonparametric discriminant analysis by Ghosh and Chaudhuri [2005]. Mizera and Müller [2004] defined and studied the location-scale depth and gave some statistical applications.

List of tables and figures

Table 1: Depth values and *de*-classes for the flood peak-volume data set (Ashuapmushuan)

Year	Q (m^3/s)	V (day m^3/s)	Oja		Tukey		Liu		Mahalanobis	
			Depth	de-class	Depth	de-class	Depth	de-class	Depth	de-class
1969	1380	50895	2.84E-07	1	0.3939	1	0.3310	1	0.9824	1
1973	1470	55766	2.75E-07	2	0.3636	2	0.3248	2	0.9211	2
1975	1260	48790	2.62E-07	3	0.3030	4	0.2980	4	0.8236	4
1984	1460	57769	2.58E-07	4	0.3333	3	0.3021	3	0.8023	5
1995	1550	51853	2.56E-07	5	0.3030	4	0.2892	5	0.8319	3
1993	1360	45263	2.50E-07	6	0.3030	4	0.2757	6	0.7436	6
1985	1210	47627	2.46E-07	7	0.2424	5	0.2515	7	0.7341	7
1976	1490	60767	2.31E-07	8	0.2121	6	0.2482	8	0.6420	9
1966	1650	54139	2.27E-07	9	0.2121	6	0.2368	9	0.6860	8
1972	1160	42497	2.22E-07	10	0.1818	7	0.2346	10	0.5794	10
1991	1130	49226	2.04E-07	11	0.1212	8	0.1683	12	0.5625	11
1978	1530	63663	2.03E-07	12	0.1818	7	0.1877	11	0.5121	12
1977	1370	60824	1.95E-07	13	0.0909	9	0.1602	14	0.5043	13
1981	1500	64631	1.88E-07	14	0.0909	9	0.1290	19	0.4478	14
1989	1490	41943	1.85E-07	15	0.1212	8	0.1606	13	0.4216	15
1965	1330	38682	1.81E-07	16	0.0909	9	0.1290	19	0.4161	16
1968	1100	37213	1.80E-07	17	0.0909	9	0.1345	17	0.3991	17
1983	1590	67223	1.72E-07	18	0.0909	9	0.1158	22	0.3900	19
1988	993	36882	1.69E-07	19	0.0909	9	0.1246	20	0.3498	23
1970	1780	66879	1.69E-07	20	0.0909	9	0.1437	15	0.3983	18
1986	1690	46735	1.68E-07	21	0.0909	9	0.1290	19	0.3667	20
1971	1420	38634	1.67E-07	22	0.0606	10	0.1107	23	0.3562	21
1967	934	39744	1.63E-07	23	0.0606	10	0.1294	18	0.3417	24
1992	1820	51752	1.59E-07	24	0.0909	9	0.1426	16	0.3411	25
1964	1780	68828	1.59E-07	25	0.0606	10	0.1184	21	0.3525	22
1980	949	33010	1.47E-07	26	0.0303	11	0.0909	25	0.2751	26
1990	1570	38568	1.39E-07	27	0.0303	11	0.0909	25	0.2553	27
1882	1920	50525	1.30E-07	28	0.0303	11	0.0909	25	0.2331	29
1979	2040	59254	1.25E-07	29	0.0606	10	0.0964	24	0.2368	28
1963	968	58538	1.12E-07	30	0.0606	10	0.0964	24	0.1953	30
1987	610	35600	1.07E-07	31	0.0303	11	0.0909	25	0.1626	31
1994	1170	74840	8.50E-08	32	0.0303	11	0.0909	25	0.1073	32
1974	2400	84198	8.10E-08	33	0.0303	11	0.0909	25	0.1027	33

Table 2: Location parameters (Ashuapmushuan)

		(Q, V)		(D, V)		(Q, D)	
Mean		1.43E+03	5.22E+04	84.3	5.22E+04	1.43E+03	84.3
Trimmed mean 5%	**Tukey**	1.43E+03	5.22E+04	84.2	5.22E+04	1.43E+03	84.0
	Oja	1.41E+03	5.08E+04	83.3	5.08E+04	1.41E+03	83.3
	Mahalanobis	1.41E+03	5.08E+04	83.3	5.08E+04	1.41E+03	83.3
	Liu	1.43E+03	5.22E+04	84.2	5.22E+04	1.43E+03	84.0
Trimmed mean 10%	**Tukey**	1.43E+03	5.21E+04	84.1	5.21E+04	1.43E+03	83.6
	Oja	1.43E+03	5.09E+04	81.8	4.99E+04	1.43E+03	82.4
	Mahalanobis	1.43E+03	5.09E+04	82.4	5.08E+04	1.43E+03	82.4
	Liu	1.43E+03	5.21E+04	84.1	5.21E+04	1.43E+03	83.6
Median	**Componentwise**	1.46E+03	5.09E+04	80.0	5.09E+04	1.46E+03	80.0
	Tukey	1.41E+03	5.13E+04	81.0	5.03E+04	1.40E+03	81.0
	Oja	1.40E+03	5.15E+04	80.0	5.03E+04	1.43E+03	81.0
	Mahalanobis	1.38E+03	5.09E+04	83.0	4.88E+04	1.49E+03	84.0
	Liu	1.38E+03	5.09E+04	80.0	5.09E+04	1.38E+03	80.0
	Spacial	1.50E+03	5.09E+04	80.0	5.09E+04	1.46E+03	84.0

Table 3: Dispersion matrices (Ashuapmushuan)

		(Q, V)		**(D, V)**		**(Q, D)**	
Dispersion (0%)		1.29E+05	2.67E+06	2.11E+02	1.03E+05	1.29E+05	-9.56E+02
		2.67E+06	1.55E+08	1.03E+05	1.55E+08	-9.56E+02	2.11E+02
Trimmed dispersion 5%	**Tukey**	1.25E+05	2.75E+06	1.64E+02	7.39E+04	9.60E+04	-6.32E+02
		2.75E+06	1.36E+08	7.39E+04	1.35E+08	-6.32E+02	2.09E+02
	Oja	1.00E+05	1.81E+06	1.68E+02	7.33E+04	1.13E+05	-5.60E+02
		1.81E+06	1.13E+08	7.33E+04	1.20E+08	-5.60E+02	1.58E+02
	Mahalanobis	1.00E+05	1.81E+06	1.79E+02	9.03E+04	1.16E+05	-4.92E+02
		1.81E+06	1.13E+08	9.03E+04	1.16E+08	-4.92E+02	1.59E+02
	Liu	1.18E+05	2.73E+06	2.29E+02	1.08E+05	9.47E+04	-5.97E+02
		2.73E+06	1.52E+08	1.08E+05	1.36E+08	-5.97E+02	2.28E+02
Trimmed dispersion 10%	**Tukey**	1.13E+05	2.47E+06	1.62E+02	7.78E+04	8.66E+04	-3.82E+02
		2.47E+06	1.30E+08	7.78E+04	1.22E+08	-3.82E+02	1.98E+02
	Oja	8.37E+04	1.61E+06	1.28E+02	6.07E+04	8.62E+04	-1.15E+02
		1.61E+06	1.04E+08	6.07E+04	1.08E+08	-1.15E+02	1.53E+02
	Mahalanobis	8.37E+04	1.61E+06	1.52E+02	8.29E+04	8.65E+04	-1.24E+02
		1.61E+06	1.04E+08	8.29E+04	1.06E+08	-1.24E+02	1.54E+02
	Liu	1.04E+05	2.51E+06	2.23E+02	1.12E+05	8.46E+04	-3.04E+02
		2.51E+06	1.34E+08	1.12E+05	1.09E+08	-3.04E+02	2.18E+02

Table 4: Outlier detection for the three considered bivariate series using Mahalanobis, Spatial and Tukey outlyingness with normal and empirical thresholds (Ashuapmushuan)

			Mahalanobis	**Spatial**	**Tukey**
(Q, V)	Normal	Threshold	0.7297	---	0.9931
		Outliers (years)	1989-1995	---	None
	Empirical	Threshold	0.8973	0.9695	0.9394
		Outliers (years)	None	None	None
(D, V)	Normal	Threshold	0.7297	---	0.9931
		Outliers (years)	1982;1988; 1990-1995	---	None
	Empirical	Threshold	0.9181	0.9697	0.9394
		Outliers (years)	None	None	None
(Q, D)	Normal	Threshold	0.7297	---	0.9931
		Outliers (years)	1986;1988; 1990-1995	---	None
	Empirical	Threshold	0.8921	0.9695	0.9394
		Outliers (years)	None	None	None

Table 5: Tukey depth and outlyingness values for the flood peak-volume series (Magpie)

Year	Q	V	Tukey Depth	O_{MD}	O_S	O_{HD}
1979	886.67	2088.92	0.2692	0.0571	0.1361	0.4615
1980	849.67	2357.02	0.3846	0.1971	0.1567	0.2308
1981	1456.67	3909.14	0.0385	**0.8851**	**0.9563**	**0.9231**
1982	1270.00	2443.15	0.0385	0.8032	0.6246	**0.9231**
1983	974.67	3012.18	0.0769	0.6700	0.8500	0.8462
1984	1056.67	2751.69	0.1154	0.4713	0.6857	0.7692
1985	787.00	1574.21	0.1538	0.4623	0.4815	0.6923
1986	610.33	1536.34	0.1154	0.5306	0.6026	0.7692
1987	344.33	1069.86	0.0385	0.8225	0.9204	**0.9231**
1988	843.33	2374.49	0.3077	0.2390	0.2455	0.3846
1989	678.67	1534.53	0.1923	0.4534	0.5395	0.6154
1990	506.33	1752.06	0.0769	0.7223	0.5603	0.8462
1991	740.00	2260.57	0.1538	0.4461	0.3003	0.6923
1992	710.80	1128.71	0.0385	0.7223	0.8923	**0.9231**
1993	666.80	1407.32	0.1538	0.5400	0.6964	0.6923
1994	932.90	2722.55	0.1538	0.4802	0.6113	0.6923
1995	868.77	2192.44	0.3462	0.0068	0.0324	0.3077
1996	886.90	2476.36	0.3077	0.2644	0.3562	0.3846
1997	697.30	2665.87	0.0385	0.7817	0.6607	**0.9231**
1998	825.00	1843.60	0.3077	0.1963	0.2717	0.3846
1999	1306.67	2652.26	0.0385	0.8042	0.7450	**0.9231**
2000	858.90	2492.65	0.2308	0.3526	0.4095	0.5385
2001	732.50	1188.92	0.0769	0.7053	0.8076	0.8462
2002	999.60	1485.36	0.0385	0.8045	0.6758	**0.9231**
2003	1004.93	1883.80	0.1538	0.6236	0.4102	0.6923
2004	842.57	2802.32	0.0769	0.6783	0.7252	0.8462

Bold character indicates outlyingness of the detected outliers

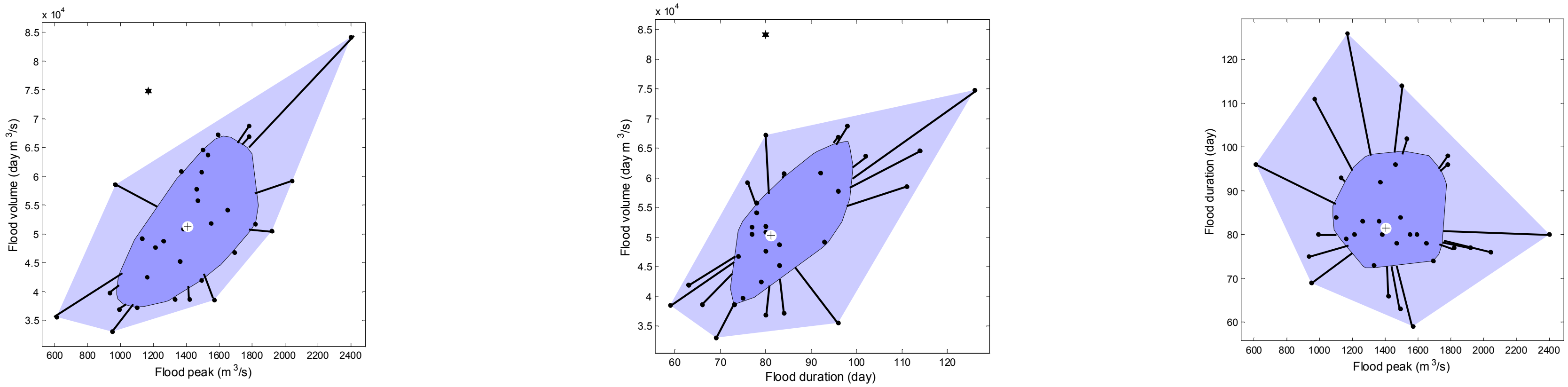

Figure 1a : Bagplots using Tukey depth : (Q, V) left, (D, V) middle and (Q, D) right (Ashuapmushuan)

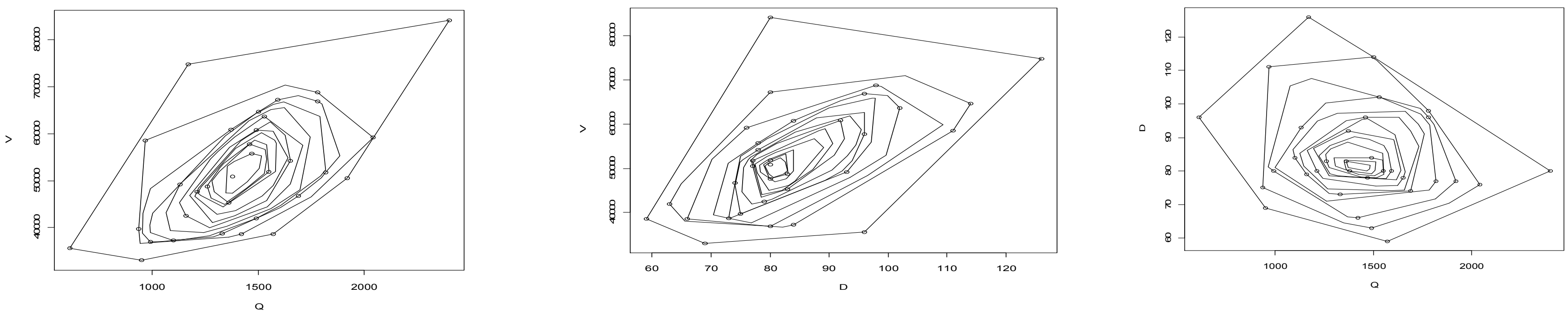

Figure 1b : Contour plots using Tukey depth : (Q, V) left, (D, V) middle and (Q, D) right (Ashuapmushuan)

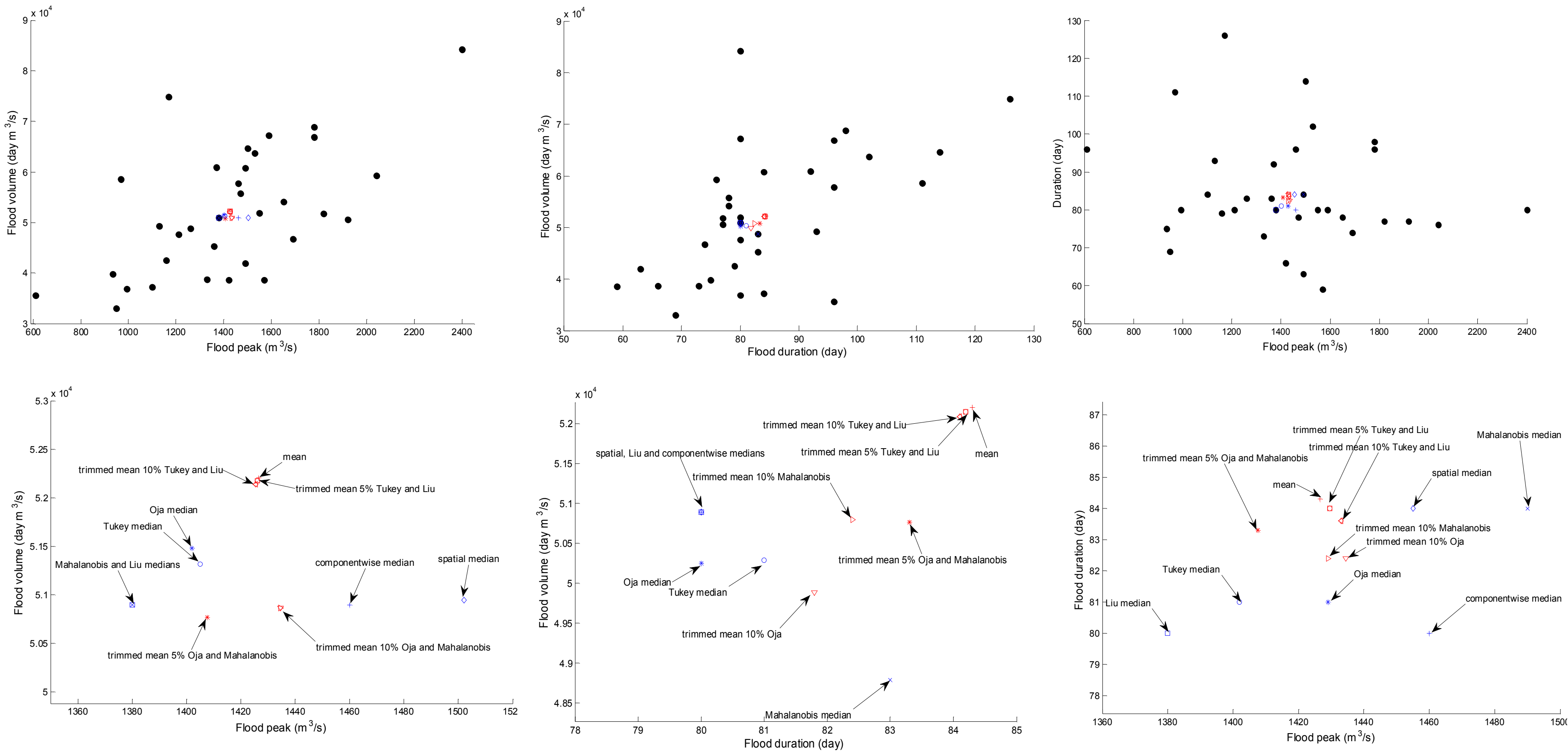

Figure 2: Location parameters: (Q, V) left, (D, V) middle and (Q, D) right. Top figures present the location parameters within the data and in the bottom figures a zoom is made to show the different location parameters (Ashuapmushuan)

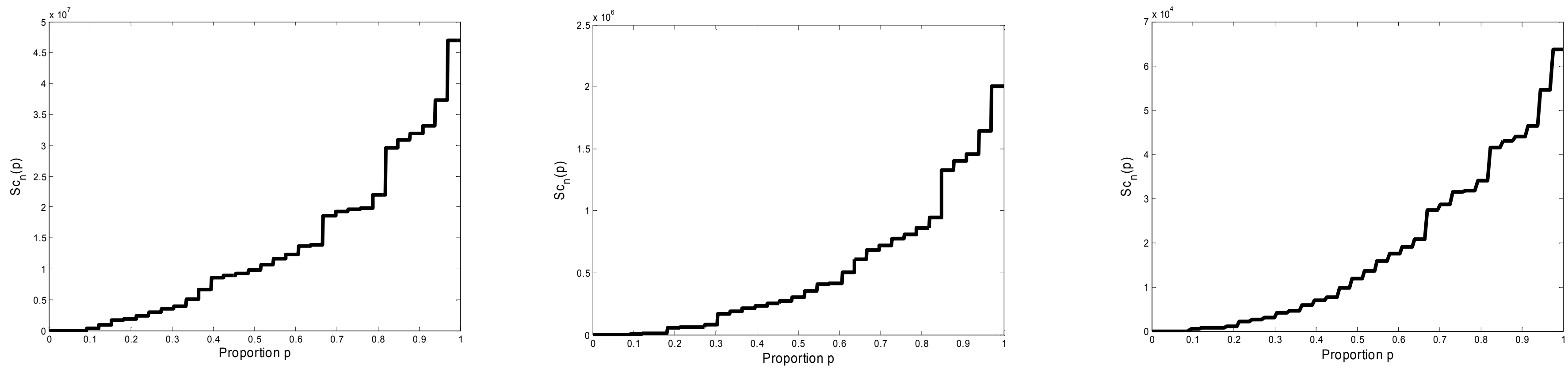

Figure 3 : Scalar scales using Tukey depth : (Q, V) left, (D, V) middle and (Q, D) right (Ashuapmushuan)

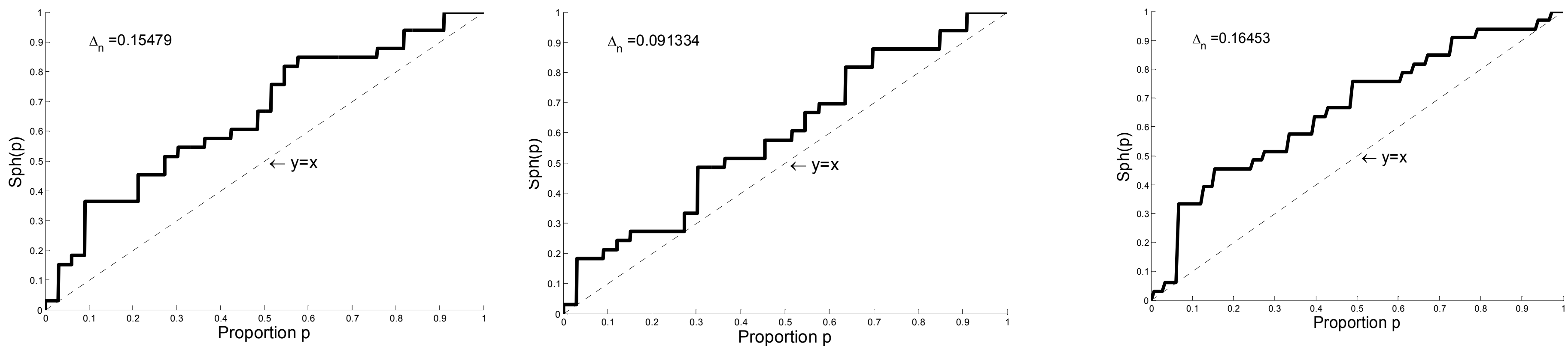

Figure 4a : Spherical skewness using Tukey depth : (*Q*, *V*) left, (*D*, *V*) middle and (*Q*, *D*) right (Ashuapmushuan)

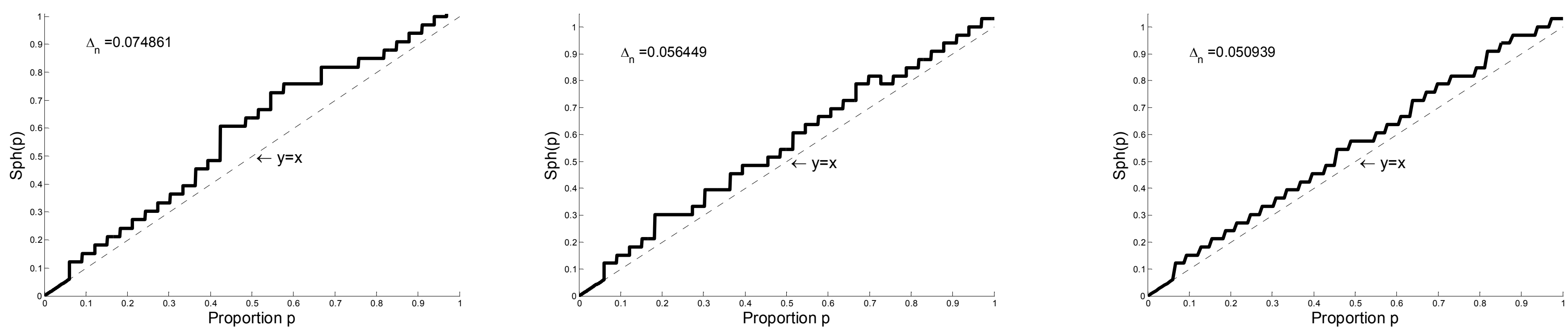

Figure 4b : Elliptical skewness using Tukey depth: (*Q*, *V*) left, (*D*, *V*) middle and (*Q*, *D*) right (Ashuapmushuan)

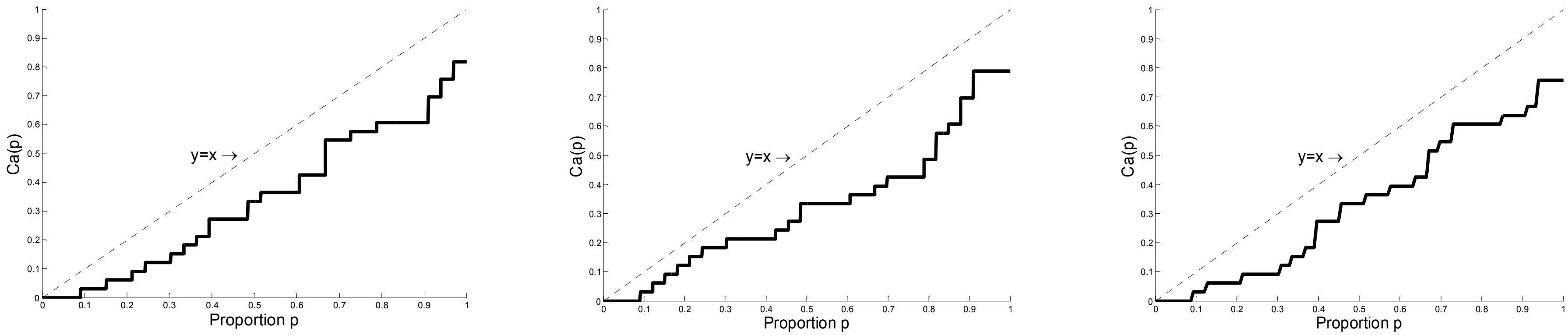

Figure 4c : Antipodal skewness using Tukey depth : (Q, V) left, (D, V) middle and (Q, D) right (Ashuapmushuan)

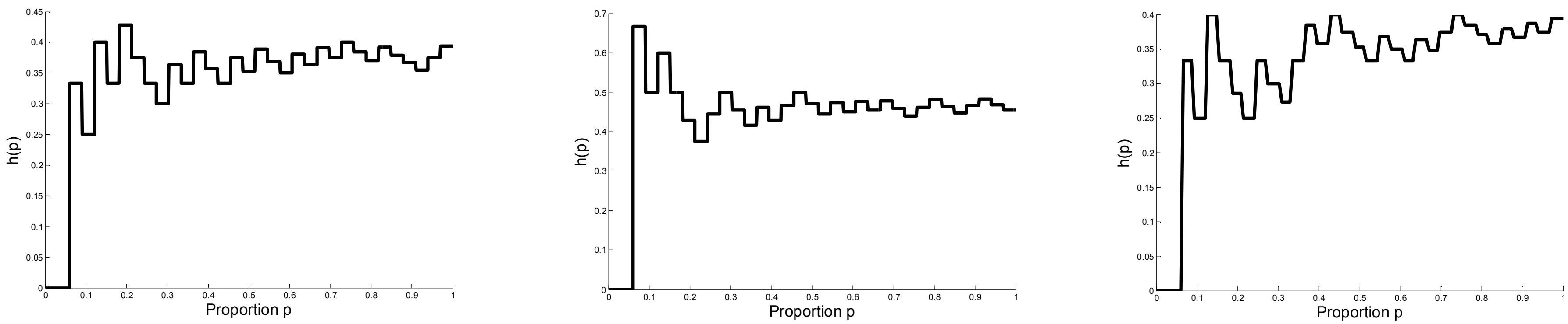

Figure 4d : Angular skewness using Tukey depth : (Q, V) left, (D, V) middle and (Q, D) right (Ashuapmushuan)

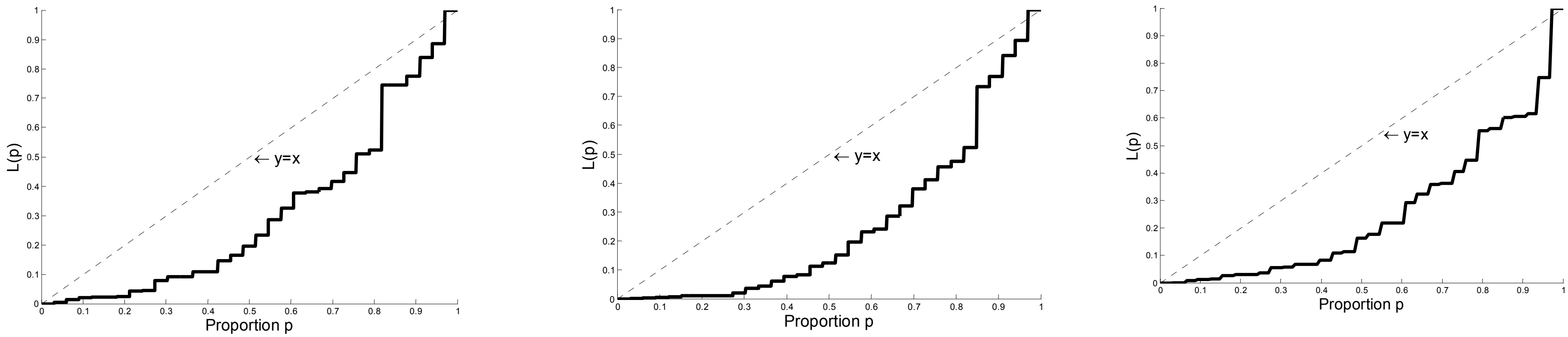

Figure 5a : Kurtosis measure with L(p) using Tukey depth : (*Q*, *V*) left, (*D*, *V*) middle and (*Q*, *D*) right (Ashuapmushuan)

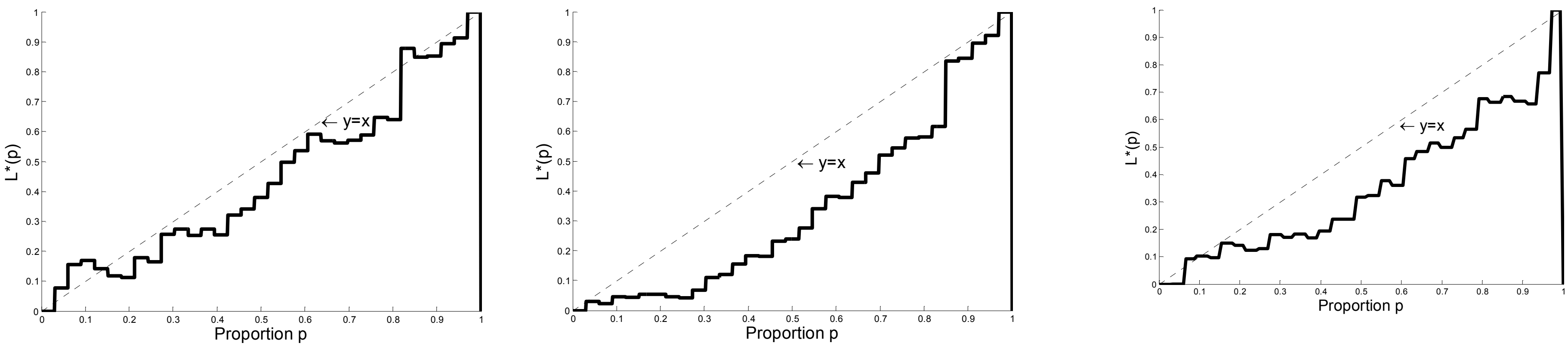

Figure 5b : Kurtosis measure with L*(p) using Tukey depth : (*Q*, *V*) left, (*D*, *V*) middle and (*Q*, *D*) right (Ashuapmushuan)

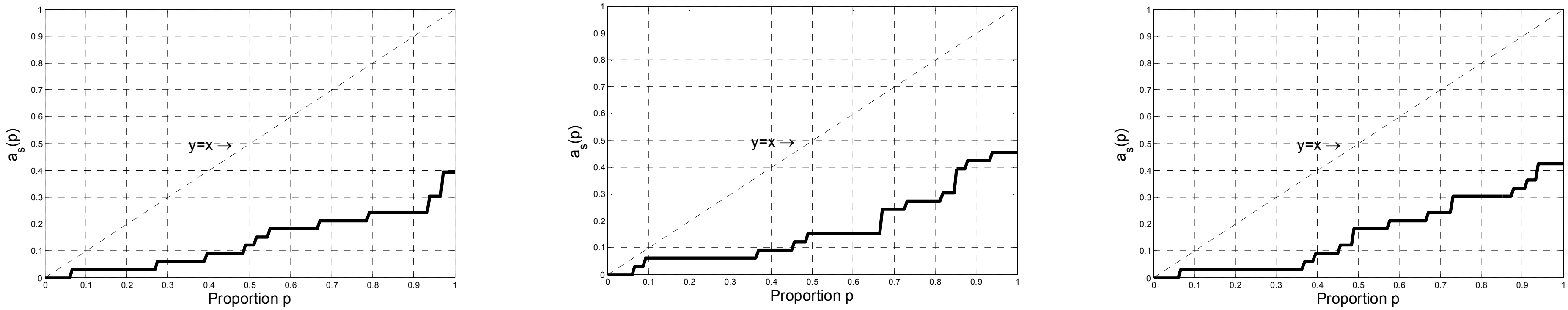

Figure 5c : Kurtosis measure with shrinkage using Tukey depth : (*Q*, *V*) left, (*D*, *V*) middle and (*Q*, *D*) right (Ashuapmushuan)

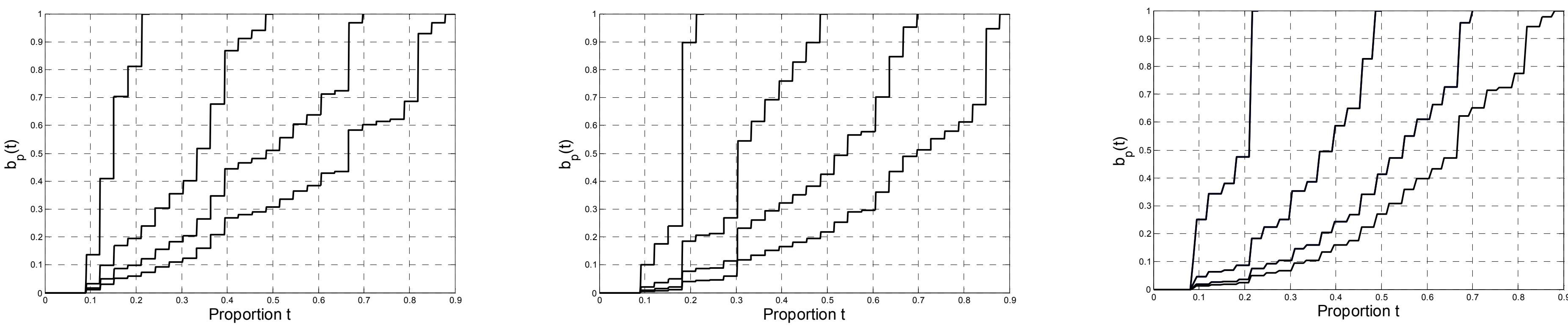

Figure 5d : Kurtosis measure with fan plots using Tukey depth : (*Q*, *V*) left, (*D*, *V*) middle and (*Q*, *D*) right (Ashuapmushuan)

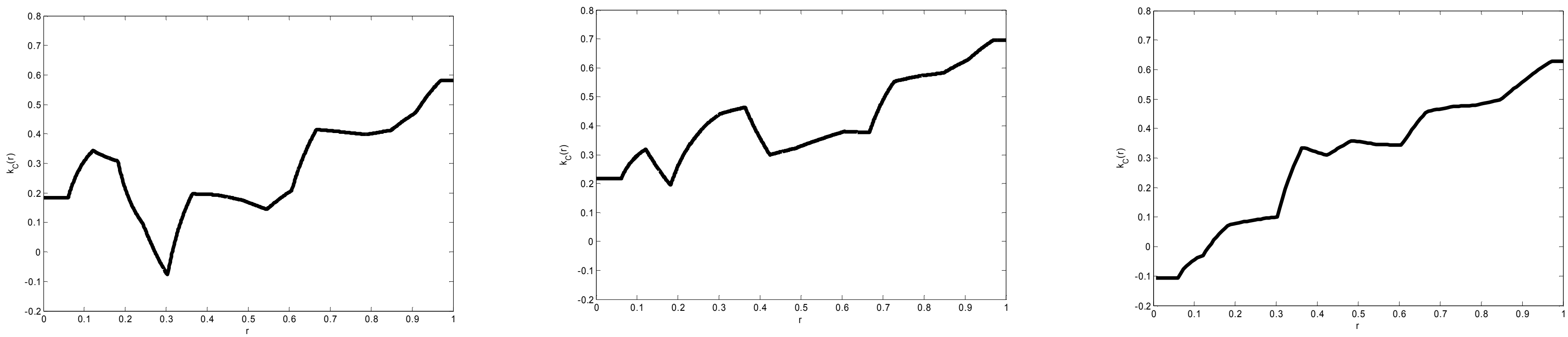

Figure 5e : Kurtosis measure with quantile using Tukey depth : (Q, V) left, (D, V) middle and (Q, D) right (Ashuapmushuan)

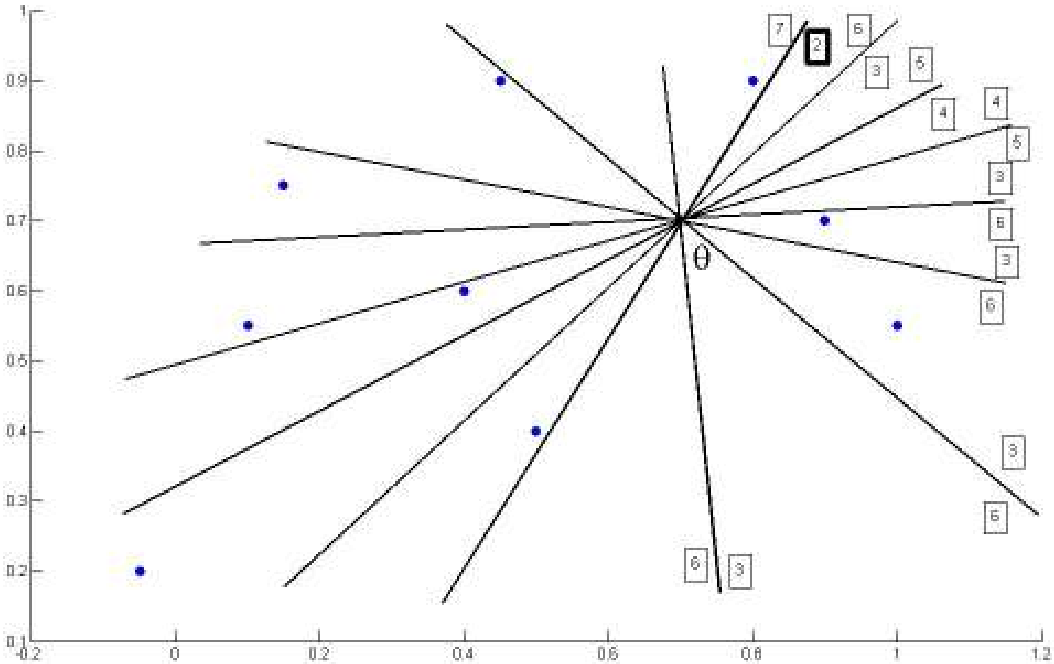

Figure 6: Half-space depth evaluation for the point θ in an arbitrary generated sample. The numbers in boxes represent the number of points in the associated half-space. The minimum value is 2 which gives the depth value of θ which is equal to as 2 divided by the sample size.